



RESEARCH PAPER

The CA domain of the respiratory complex I is required for normal embryogenesis in *Arabidopsis thaliana*

Juan Pablo Córdoba, Fernanda Marchetti, Débora Soto, María Victoria Martín¹, Gabriela Carolina Pagnussat and Eduardo Zabaleta*

Instituto de Investigaciones Biológicas IIB-CONICET-UNMdP, Funes 3250 3er nivel 7600 Mar del Plata, Argentina

¹ Present address: Instituto de Investigaciones en Biodiversidad y Biotecnología (INBIOTEC-CONICET), Fundación para Investigaciones Biológicas Aplicadas (CIB-FIBA), Vieytes 3103, 7600 Mar del Plata, Argentina

* To whom correspondence should be addressed. E-mail: ezabalet@mdp.edu.ar

Received 6 October 2015; Revised 24 November 2015; Accepted 10 December 2015

Editor: Steve Penfield, John Innes Centre

Abstract

The NADH-ubiquinone oxidoreductase [complex I (CI), EC 1.6.5.3] of the mitochondrial respiratory chain is the principal entry point of electrons, and vital in maintaining metabolism and the redox balance. In a variety of eukaryotic organisms, except animal and fungi (Opisthokonta), it contains an extra domain composed of putative gamma carbonic anhydrases subunits, named the CA domain, which was proposed to be essential for complex I assembly. There are two kinds of carbonic anhydrase subunits: CAs (of which there are three) and carbonic anhydrase-like proteins (CALs) (of which there are two). In plants, the CA domain has been linked to photorespiration. In this work, we report that *Arabidopsis* mutant plants affected in two specific CA subunits show a lethal phenotype. Double homozygous knockouts *ca1ca2* embryos show a significant developmental delay compared to the non-homozygous embryos, which show a wild-type (WT) phenotype in the same silique. Mutant embryos show impaired mitochondrial membrane potential and mitochondrial reactive oxygen species (ROS) accumulation. The characteristic embryo greening does not take place and fewer but larger oil bodies are present. Although seeds look dark brown and wrinkled, they are able to germinate 12 d later than WT seeds. However, they die immediately, most likely due to oxidative stress.

Since the CA domain is required for complex I biogenesis, it is predicted that in *ca1ca2* mutants no complex I could be formed, triggering the lethal phenotype. The *in vivo* composition of a functional CA domain is proposed.

Key words: Embryogenesis, gamma carbonic anhydrase, membrane potential, reactive oxygen species, respiration, respiratory complex I.

Introduction

Complex I (CI) (NADH-ubiquinone oxidoreductase, EC 1.6.5.3) is the largest complex of the mitochondrial or bacterial respiratory chain. It catalyzes the transfer of two electrons from NADH to quinone coupled to proton translocation across the membrane. In many systems it represents the major entry point of electrons from metabolism (Gray, 2012). In bacteria, it contains 14 subunits (Friedrich, 1998). Eukaryotic

CI contains additional 31–38 proteins named ‘accessory subunits’, some of them differing among species (Bridges *et al.*, 2010; Cardol, 2011; Andrews *et al.*, 2013; Peters *et al.*, 2013; Braun *et al.* 2014). A specific matrix-exposed domain formed by γ -carbonic anhydrase (CA) subunits attached to the membrane arm of the complex was identified by using single particle electron microscope analyses in *Arabidopsis*

(Dudkina *et al.*, 2005; Sunderhaus *et al.*, 2006). By using a proteomic approach, the CA domain was shown to contain at least two different γ -CA proteins, CA1 (At1g19580) and CA2 (At1g47260), which show conserved active site regions, and two less well conserved γ -CA-like proteins: CAL1 (At5g63510) and CAL2 (At3g48680) (Klodmann *et al.*, 2010). However, it has been suggested that the CA domain is arranged as a trimer (Perales *et al.*, 2004; Sunderhaus *et al.*, 2006). A third CA protein (CA3; At5g66510) was not found in the CA domain although it is considered a CI subunit (Klodmann *et al.*, 2010). Thus, the exact composition of the CA domain is currently unknown.

CA subunits were first thought to be specific components of the CI from photosynthetic organisms (Heazlewood *et al.*, 2003; Parisi *et al.*, 2004). However, further investigations demonstrated that homologous γ -CA proteins exist in the CI isolated from a range of other eukaryotic lineages including slime moulds and amoebae that lack photosynthesis (Gawryluk and Gray, 2010). Up to now, it was not detected in animals and fungi. A role for the CA domain in CI biogenesis was experimentally proven in Arabidopsis (Klodmann *et al.*, 2010; Meyer *et al.*, 2011; Li *et al.*, 2013). Additionally, specific roles in plant photomorphogenesis and growth including male sterility have been shown by gene knockout studies (Wang *et al.*, 2012) and by overexpression of the CA2 subunit (Villarreal *et al.*, 2009). This subunit is probably the most important for CI biogenesis, since *ca2* mutants show 80% less CI than WT plants. The CA2 protein was also proposed to bind inorganic carbon ($\text{Ci} = \text{HCO}_3^-$ and CO_2 ; Martin *et al.*, 2009). Accordingly, it has been postulated that the CA domain might be involved in recycling CO_2 from respiration and photorespiration (Braun and Zabaleta, 2007; Zabaleta *et al.*, 2012). Experimental data recently published support a link of this domain with photorespiration (Soto *et al.*, 2015).

Several mutants showing complex I defects have been characterized in Arabidopsis. These include knockout mutants of complex I subunits (Perales *et al.*, 2005; Meyer *et al.*, 2009, Kühn *et al.*, 2015; Soto *et al.*, 2015) or mutants that lack proteins affecting the expression of complex I subunits [summarized in Colas de Francs-Small and Small (2014)]. These mutants show a range of altered growth phenotypes, from WT-like to severe delayed growth, which might be attributable to variable amounts of complex I, different subcomplex accumulation or lack of NADH dehydrogenase activity. The role of complex I during seed development however, is still unclear. Arabidopsis mutants with undetectable complex I, like *organelle transcript processing defect43* (*otp43*) defective in a pentatricopeptide repeat (PPR) protein show curled leaves and an extremely delayed growth *in vitro*, producing malformed seeds that do not germinate. OTP43 is involved in the trans-splicing of the mitochondrial *nad1*, although it is not clear whether subcomplexes are present in this mutant (de Longevialle *et al.*, 2007). Another mutant that is defective in complex I activity, *ndufv1*, which lacks a *bona fide* component of the complex (NADH-binding subunit NDUFV1), requires sugar for germination and accumulates partially assembled complex I (Kühn *et al.*, 2015). In other plant species, mutants in complex I subunits have been characterized, such as the

conditional mutant CMSII of *Nicotiana sylvestris* (Pineau *et al.*, 2005) and *nonchromosomal stripe2* (NCS2) in *Zea mays* (Karpova and Newton, 1999). Both mutants show partially assembled complex I due to the lack of essential subunits (NAD7 or a PPR affecting *nad4* transcript, respectively). However, phenotypes are different presenting delayed growth and photosynthesis deficiency (Dutilleul *et al.*, 2003) or lethality during kernel development (Karpova and Newton, 1999). Moreover, the corresponding mutant in Arabidopsis produces seeds that germinate at low rates (Haili *et al.*, 2013).

In this report, we present experimental evidence that the CA domain of plant complex I is required for normal embryogenesis. Double knockout mutants lacking two CA subunits (*calca2* double mutants) display a significant delay in embryogenesis, embryos with low mitochondrial potential, ROS accumulation and a lethal phenotype. Although the abnormal seeds produced are able to germinate with a significant delay, mutant seedlings die shortly afterwards. As a result of interaction studies and the lethal phenotype of this particular combination of mutants we propose a model for the *in vivo* composition of the conserved CA domain in plants. This model suggests that in plant mitochondria there are different types of complex I according to the composition of their CA domains, with presumably specific physiological functions.

Materials and methods

Plant material and growth conditions

Arabidopsis thaliana ecotype Columbia (Col-0) and mutants were grown under long-day conditions (16/8h light/dark), 100 μmol quanta (μE) m^{-2} s^{-1} light intensity and a constant temperature of 22°C. After sowing, seeds were maintained in darkness at 4°C for 2 d. Single mutants *cal* (SALK_109391) and *ca2* (SALK_010194) were cross-pollinated to obtain double heterozygous mutants *calCA1ca2ca2* and *calcalca2CA2*. Growth on plates was conducted on Murashige and Skoog medium (Sigma), supplemented with 30 $\mu\text{g}/\text{ml}$ kanamycin. Seeds were previously sterilized on SDS-sodium hypochlorite solution and washed five times with sterile water.

Genotyping of heterozygous lines

Detection of insertional T-DNA on double mutant lines was performed by genomic PCR methods (previous heating of 5 min at 94°C; 30 cycles of 50 s at 94°C, 30 s at 50°C and 1 min at 72°C and final elongation step of 3 min at 72°C), using specific primers for the insertion (LBb1.3 5'-ATTTTGCCGATTTTCGGAAC-3') and for the specific gene (CA1 LP 5'-ATCTCGAGATGGGAACCCTAGGCA-3'; CA2LP 5'-CACTCGAGTGGGAACCCTAGGA-3'). Double mutant plants, heterozygous for CA1 or CA2 were allowed to self-pollinate and progeny was germinated on plates and genotyped as indicated above. Non-disrupted alleles were detected by combination of primer pairs: CA1 forward, 5'-ATCTCGAGATGGGAACCCTAGGCA-3' and CA1 reverse, 5'-TTTCCCGGGGTTACATTAGAAGGACG-3'; or CA2 forward, 5'-CACTCGAGTGGGAACCCTAGGA-3' and CA2 reverse, 5'-TCAGAGTAGGTAGAACCTTGCCA-3'.

Phenotype analysis

WT and mutant (*calCA1ca2ca2* or *calcalca2CA2*) siliques at different stages (corresponding to different stages of embryogenesis;

Bowman *et al.*, 1994) were mounted on glass slides and cleared for 16 h on Hoyer's solution. After clearing, embryos were visualized on a Zeiss Axioplan Imager-A2 microscope under differential interference contrast (DIC) optics. Images were captured with an AxioCam HRC charge-coupled device camera (Zeiss) using the Axiovision program (version 3.1). Seeds were examined by scanning electron microscopy (SEM), using a JEOL JSM-6460LV microscope.

Mitochondrial membrane potential

To analyze the mitochondrial membrane state, tetramethylrhodamine (TMRM) (Molecular Probes) was used. Immature pistils were emasculated and pollinated manually. After indicated times, siliques were harvested, the embryos were isolated from seed coats and incubated with 200 nM TMRM on 0.5× MS medium, 3% sucrose. After 30 min incubation, seeds were mounted with buffer and images were taken using a confocal microscope (Nikon Eclipse C1 Plus). Red (excitation/emission wavelength = 485/590 nm) fluorescence was analyzed for 100 ovules or embryos from WT and mutant plants. Quantification was performed as described (Martin *et al.*, 2013).

Mitochondrial density

Active mitochondria density was determined using MitoTracker Red CM-H2Xros dye (Molecular Probes). Stock solution was prepared according to the supplier's indications, and used at a final concentration of 10 μM. Staining and mounting protocols were the same as above. Visualization of red fluorescence was performed in a confocal microscope (Nikon Eclipse C1 Plus).

Reactive oxygen species detection

To detect hydrogen peroxide diaminobenzidine (DAB; Sigma) staining was used. Briefly, siliques and pistils were vacuum-infiltrated (three times for 5 min) with a DAB solution (1 mg ml⁻¹). After overnight incubation at room temperature in total darkness, samples were dissected and cleared for 16 h in Hoyer's solution.

Detection of superoxide was performed by nitroblue tetrazolium (NBT) staining. Siliques and pistils were vacuum-infiltrated (three times for 5 min) in a 10 mM phosphate buffer, pH 7.8, containing 10 mM NaN₃ and 0.1% NBT (Promega) and incubated in darkness overnight at 37°C. Samples were dissected and cleared for 16 h in Hoyer's solution.

Mitochondrial superoxide and general ROS were detected by MitoSOX red and H₂DCFDA (Molecular Probes), respectively. MitoSOX red was used at 5 μM in 20 mM HEPES buffer, pH 7.2. H₂DCFDA was used at 10 μM in the same buffer. Siliques and pistils were dissected and mounted with buffer, followed by confocal microscopic visualization (Nikon Eclipse C1 Plus). H₂DCFDA was excited at 488-nm line, and images were acquired with the green photomultiplier channel. For MitoSOX red, 408-nm line was used for excitation, and the red photomultiplier channel of the confocal microscope was used for image acquisition.

GUS activity stain

The CA2 promoter region (2000 bp upstream of the first translational codon) was amplified with specific primers: forward, 5'-TCTAGATAGGGTTCCCATTTTTTGTGATTCTCC-3' and reverse: 5'-TTTTCTAGACTTGAAGTAAAGTCTTCTC ACGGCGT-3', sequenced and cloned into the pBI 101.1 vector (<https://www.arabidopsis.org/>). Arabidopsis Col-0 plants were transformed with this CA2::GUS construction through the floral dip

method (Clough and Bent, 1998). β-glucuronidase activity staining was performed as follows: siliques at different stages of maturation (corresponding to different stages of embryogenesis) were collected, split longitudinally and then fixed in 90% acetone at -20°C for 30 min. After three washes in 100 mM sodium phosphate buffer pH 7.0, tissues were stained overnight with 100 mM sodium phosphate buffer, 10 mM EDTA, 5 mM K₄Fe(CN)₆·3H₂O, 5 mM K₃Fe(CN)₆, 0.1% Triton X-100 and 1 mg ml⁻¹ 5-bromo-4-chloro-1H-indol-3-yl β-D-glucopyranosiduronic acid (X-GLUC, Biosynth) at 37°C. After incubation, tissues were cleared for 16 h on Hoyer's solution.

Neutral lipid staining

Seed oil bodies were stained with Nile Red (Sigma), a neutral lipid stain, according to Miquel *et al.* (2014) and Siloto *et al.* (2006). After staining, images were obtained by confocal microscopy on the red channel. Immature embryos were directly isolated from seeds. Dry seeds were imbibed for 48 h and embryos were isolated to perform staining.

Yeast two-hybrid analysis

CA protein interactions were examined by using the yeast two-hybrid system (Gietz *et al.*, 1992). Bait constructs were generated which expressed Gal4 fusion proteins with the entire coding sequence of CA1 or CA2 proteins. The sequences encoding these polypeptides were amplified by PCR and inserted into the EcoRI and XhoI sites immediately downstream of the Gal4 DNA-binding Domain (BD) or activation domain (AD) into the appropriate vectors (pGBKT7 and pGADT7, respectively). Yeast colonies transformed with two constructs were grown on auxotrophy media: non selective medium (-leu, -trp dropout) or selective (-leu, -trp, -his dropout), (Clontech, CA, Palo Alto, <https://www.clontech.com>) with 40 mM 3-aminotriazole (3-AT) at 30°C in the yeast strain Y190, (genotype: MATa; trp1-901; leu 2-3,112; ade2-101; ura 3-52; his 3-200; gal44512; gal804538; URA3::GAL=lacZ; LYS2::GAL(UAS)=HIS2). Growth in this medium indicates that both proteins interact. Yeast transformation was performed using the lithium acetate method (Gietz *et al.*, 1992).

Silencing strategy and transcript quantification by qPCR

An artificial microRNA (amiR) strategy was used. Two independent sequences targeting CA1 and CA2 genes were designed by Web MicroRNA designer (<http://wmd3.weigelworld.org/cgi-bin/webapp.cgi>), including the CA3 and CAL genes as 'off-targets'. These sequences were assembled into the natural miR390 and the entire sequence was synthesized (Genscript, www.genscript.com). They were subsequently cloned into the pCHF3 binary vector containing the 35S CMV promoter and transformed into *rad6* mutant plants by the floral dip method (Clough and Bent, 1998). Twenty-two independent lines were obtained with different degrees of silencing for CA1 and CA2 genes. Total RNA was extracted with TriZOL reagent (Invitrogen) and used for quantitative RT-PCR (qPCR) using Power SYBR Green PCR mix in a StepOne machine (Applied Biosystems; <http://www.lifetechnologies.com/ar>). Transcript levels were normalized against ACT2 as housekeeping gene. qPCR primer pairs were used as described (Soto *et al.*, 2015).

Membrane isolation and gel electrophoresis procedures

Isolation of membranes from green Arabidopsis plants was performed as described previously (Pineau *et al.*, 2008). 1D blue native PAGE was performed as described by Wittig *et al.* (2006). Protein solubilization for blue native PAGE was performed using digitonin at a concentration of 5 μg mg⁻¹ mitochondrial protein as described by Eubel *et al.* (2003). Blue native separation of protein complexes was performed in gradient gels of 4.5–16% polyacrylamide.

Results

Selfed ca1ca2 heterozygous plants produce a high frequency of abnormal seeds

The CA domain of respiratory complex I is composed of at least three CA subunits. However, in *Arabidopsis*, its gene family is composed of five members. None of the single mutants of each CA domain subunit (*ca1*, *ca2*, *ca3*, *ca11* or *ca12*) shows any altered phenotype, although *ca2* mutants contain 20% of complex I (Perales et al., 2005). In order to investigate the role of this domain, crosses of CA single mutants (*ca1* and *ca2*) were performed to obtain the double knockout mutant. Since double knockout plants were not identified, developing seeds from plants homozygous for one gene and heterozygous for the second gene (i.e. *ca1ca1ca2CA2* or *ca1CA1ca2ca2*) and WT selfed plants were analyzed. During *Arabidopsis* seed development, the external appearance of the immature seed changes from white to green, and then turns to light brown before seed release. Immature seeds within a single silique develop at approximately the same rate; however, in siliques of both heterozygous plants (*ca1ca1ca2CA2* and *ca1CA1ca2ca2*), a percentage of abnormal seeds appear white (immature siliques) or dark brown and wrinkled (dry

siliques) in comparison with normal green developing or pale brown seeds of the WT (Fig. 1B; Supplementary Fig. S1 available at *JXB* online; Meinke, 1994). Ten dry siliques per plant were collected and seeds were observed under a binocular and SEM microscope and scored for abnormalities in external morphology. The average frequency of abnormal seeds per silique for both heterozygous plants was 23.0%, whereas only 2.37% of seeds from siliques from WT plants were abnormal (Fig. 1C). Abnormal seed percentage seen in the heterozygous *ca1ca1ca2CA2* or *ca1CA1ca2ca2* mutant plants were similar and found to be significantly different from WT frequencies ($P < 0.05$). The proportion of abnormal seeds is consistent with a 3:1 ratio of Mendelian segregation, strongly suggesting that these abnormal seeds were the double knockout seeds. These seeds were unable to germinate over the time at which WT seeds do to produce green plants.

Double homozygous ca1ca2 embryos show delay in embryogenesis

No double homozygous plants were found by genotyping seedlings of selfed *ca1ca1ca2CA2* or *ca1CA1ca2ca2* progenies (Supplementary Fig. S2A). To further characterize

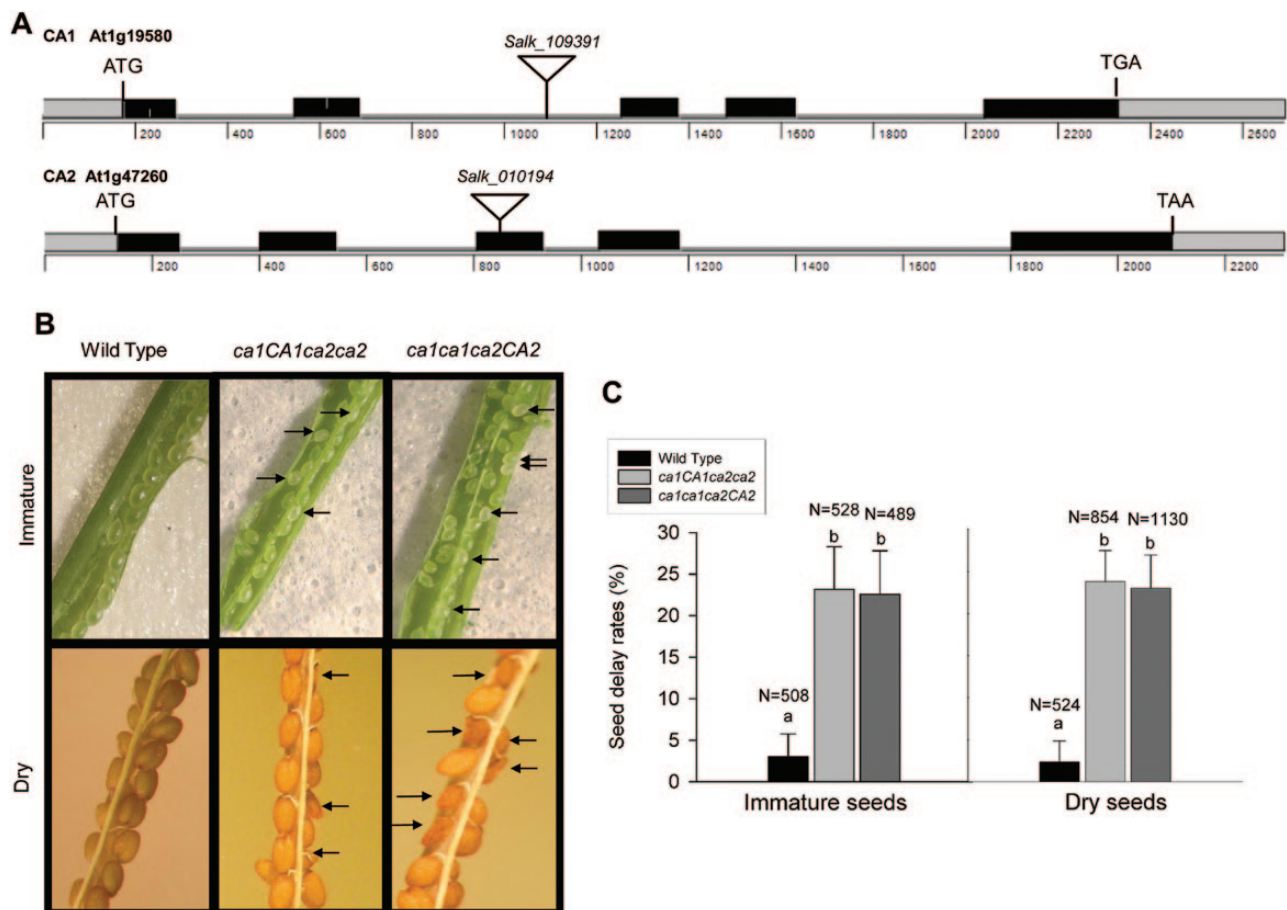


Fig. 1. Siliques of heterozygous *ca1ca1ca2CA2* and *ca1CA1ca2ca2* plants contain aborted seeds. (A) Schemes of CA1 and CA2 genes showing the T-DNA insertions. Black boxes, exons; gray boxes, UTRs; gray lines, introns; triangles, T-DNA insertion sites. (B) Immature (upper) and dry (lower) siliques containing seed abortions (arrows) in *ca1CA1ca2ca2* (middle panels) and *ca1ca1ca2CA2* (right panels) plants, compared with WT (left panels). (C) Percentages of abortions counted in WT and mutant siliques. a, b indicate statistically significant differences by one-way ANOVA ($P < 0.05$). (This figure is available in colour at *JXB* online.)

abnormal seeds, ~20 siliques at different stages of maturation were removed from five heterozygous plants for *CA2* or *CA1*, cleared as indicated in *Materials and methods* and observed under DIC microscopy. A high proportion of the selfed *calca1ca2CA2* (26.7%, $n=792$) show embryos with a delay in development. This proportion is consistent with double homozygous knockout of *CA1* and *CA2* genes causing the observed delay. In order to confirm this presumption, delayed embryos, easily recognized because of their white color, were carefully extracted from the whole seed and DNA was prepared. In parallel, green embryos were also extracted as a control. Genomic PCR using specific primers for both genes and the LB primer from the T-DNA were used. In all cases, white embryos represented the double homozygous knockouts (Supplementary Fig. S2B).

From early in development until the globular stage (60 HAP) no differences were visible compared with WT embryos ($n=396$; Fig. 2A, B, F, G). Immediately after however, a delay was evident. Fig. 2C shows a WT embryo at torpedo stage (96 HAP) whereas Fig. 2H shows a double mutant embryo at early heart stage (96 HAP). The most evident differences were observed at the end of seed development. While WT developing seeds are at green curled cotyledon stage (240 HAP; Fig. 2E), double homozygous embryos showed in Fig. 2J are at torpedo stage which is normally seen ~100 HAP (Fig. 2J, C). These and further observations from staged siliques

demonstrate that the abnormal embryos do not arrest at a single developmental time point, but appear to develop more slowly.

The CA2 promoter region is active during gametogenesis as well as during embryogenesis

In order to correlate the altered phenotypes described above with the expression pattern of the concerning genes, a fusion of 2000bp of the *CA2* promoter plus the 5'UTR including the first ATG and the *GUS* (*uidA*) reporter gene was constructed and introduced into WT Arabidopsis plants. *GUS* staining of the transformed plants is strong in both male and female gametophytes (Fig. 3A, B, D, E). Particularly, in mature pollen, the segregation between *pCA2::GUS* and WT pollen grains without stain is easily observed (Fig. 3F). In the mature female gametophyte, staining appears to be stronger at the micropylar end (egg and synergid cells in Fig. 3C). After fertilization, *GUS* activity diminishes and becomes mainly confined to the embryo proper in embryos at globular to heart stages (arrows in Fig. 3G, H, I). In mature seeds, *GUS* staining is strong, covering the entire embryo (Fig. 3J, K, L). Publicly available data on eFPBrowser (<http://bar.utoronto.ca/efp/cgi-bin/efpWeb.cgi>) are consistent with these results except for expression in the endosperm. *CA1* is shown to be expressed in a similar way, but at lower levels

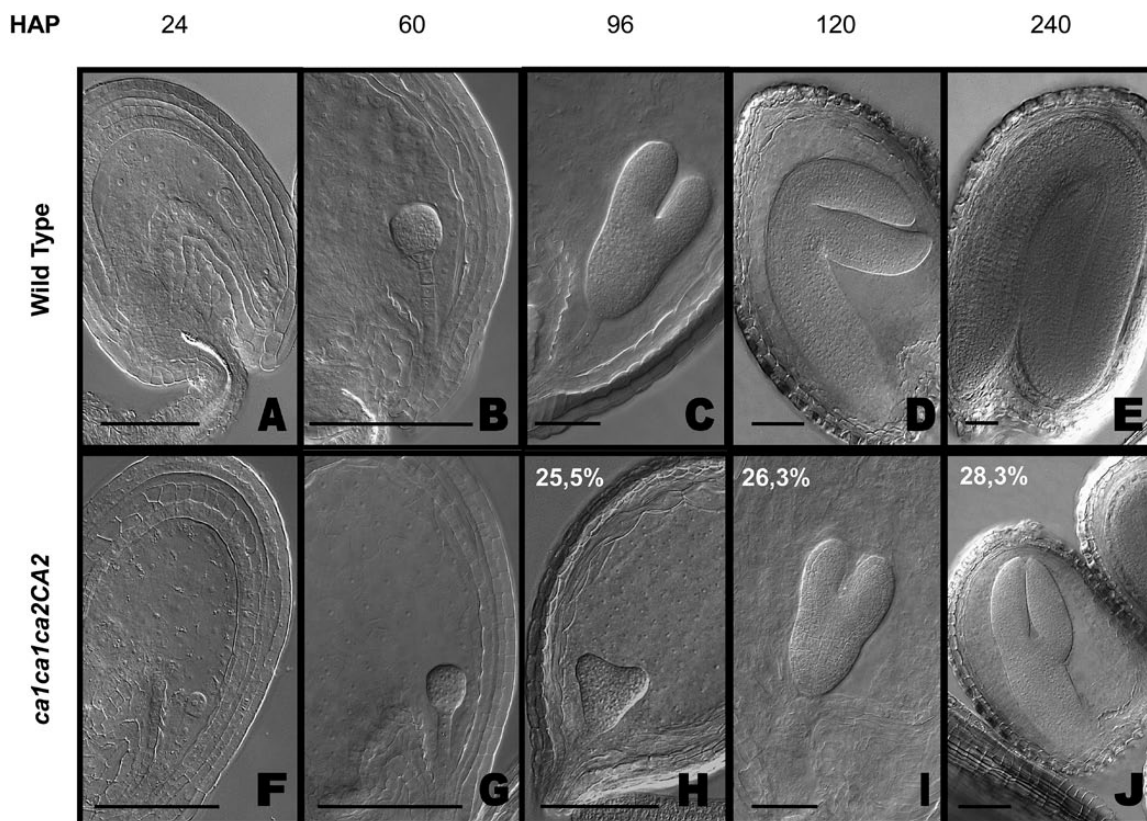


Fig. 2. Embryogenesis in WT and *ca1ca2* mutants. WT (A–E) and double mutant *ca1ca1ca2ca2* embryo developmental stages (F–J). The double mutant embryos show a growth delay, perceptible from heart stage (H) of embryogenesis. At the end of embryogenesis, these mutants are at linear cotyledon stage (J) while WT embryos are in mature green stage (E). Images were taken by DIC microscopy on embryos previously cleared 16 h in Hoyer's solution. Percentages in panels H, I and J indicate proportion of embryos in those stages, within a *ca1ca1ca2CA2* silique. H, $n=396$; I, $n=290$; J, $n=435$. Bars, 50 μm . HAP, hours after pollination.

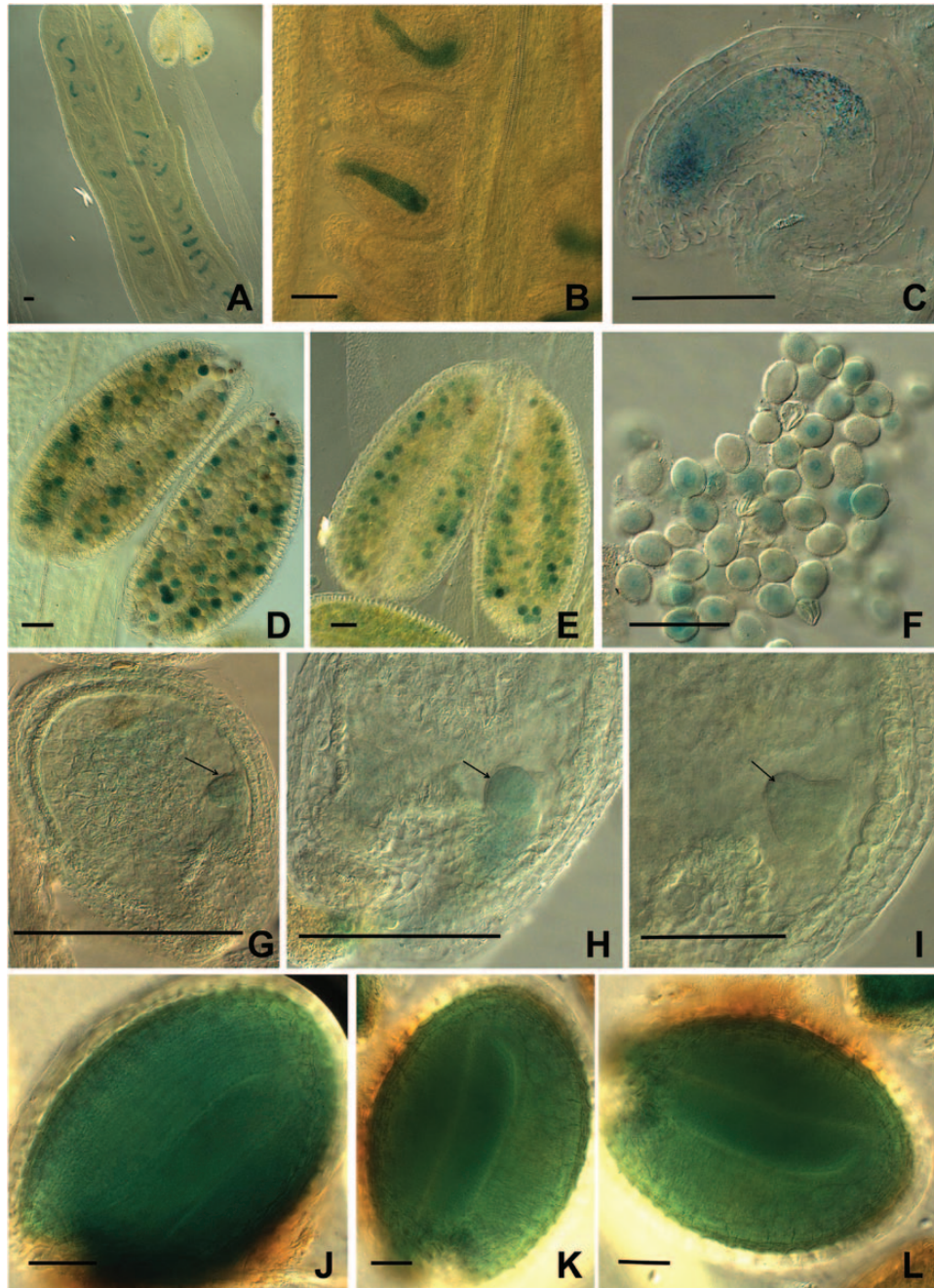


Fig. 3. Promoter activity of *CA2* gene on gametophytes and embryos. The first ATG codon of *CA2* were fused to the *GUS* (*uidA*) reporter gene 2000bp upstream and introduced into WT plants by floral dip. (A–C) Female gametophytes. (D–F) Male gametophytes. (G–I) Globular to heart stage of embryogenesis. (J–L) Green cotyledon stage of embryogenesis. Bars, 50 μ m. (This figure is available in colour at *JXB* online.)

than *CA2* which is consistent with protein levels observed in 2D blue native gels and mass spectrometry experiments in *Arabidopsis* (Perales *et al.*, 2005; Sunderhaus *et al.*, 2006; Klodmann *et al.*, 2010). Thus, both genes are expressed at the stages where altered phenotypes are visible in the mutants.

Less active mitochondria are found after the globular stage in the delayed embryos

The CA domain forms part of the complex I membrane arm. The *CA2* protein was proposed to be important for complex I biogenesis (Perales *et al.*, 2005; Meyer *et al.*, 2011), as *ca2*

mutants only contain about 20% of complex I levels. Absence of the *CA1* protein may produce a further destabilization of the remaining complex impairing respiration and thus causing a delay in embryo development. To explore this possibility, mitochondrial functional status was studied using the membrane potential ($\Delta\psi$ m) indicator TMRM, which is a cell-permeant, cationic, red-orange fluorescent dye that is readily sequestered only by active mitochondria (Brand and Nicholls, 2011). Thus, in healthy cells, red fluorescent dots correspond to active mitochondria (Mortensen *et al.*, 2010).

Mature embryo sacs and embryos at different developmental stages of both WT and *calca2CA2* plants were

examined for TMRM fluorescence under confocal microscopy (Fig. 4). Flowers were first emasculated and manually pollinated with pollen of the same plant to control developmental stages. When WT pistils were observed, embryo sacs show a strong red fluorescence (Fig. 4A), which is consistent with active mitochondria. After fertilization (12 HAP) and along embryo development, high red fluorescence remains

constant (Fig. 4C, E, G, I). When *calca1ca2CA2* pistils were analyzed, no differences were found with respect to the WT pistils until 48 HAP (Fig. 4B, D). However, when delayed embryos corresponding to *calca2* double knockouts were analyzed at 72 HAP until the end of embryogenesis, red fluorescence strongly decreased (20% of the WT; Fig. 4F, H, J). Indeed, segregating normal embryos (in *calca1ca2CA2* or

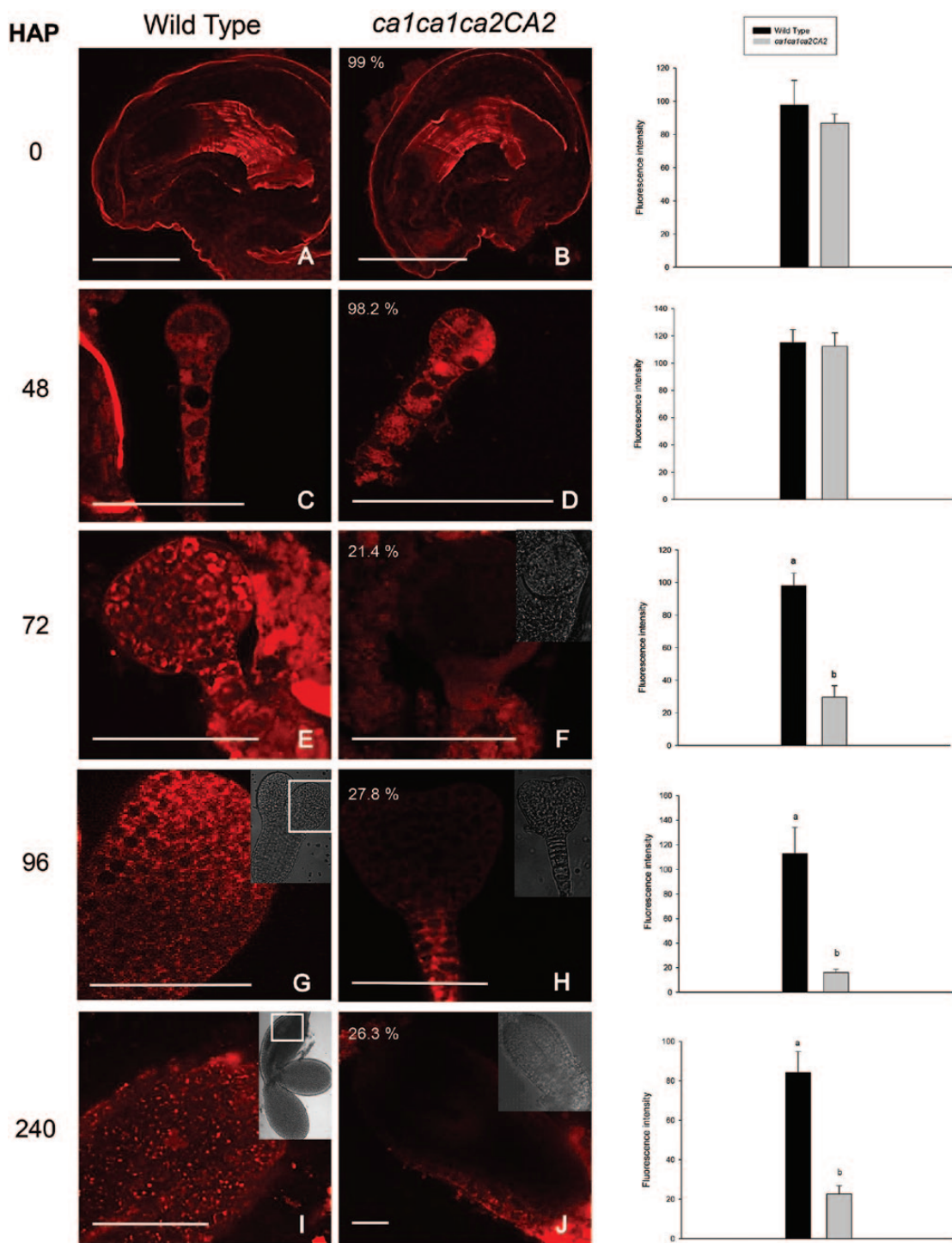


Fig. 4. Mitochondrial membrane potential in *ca1ca2* embryos decreases from globular stage. Flowers were emasculated and manually pollinated. Then, at the indicated times, embryos were extracted from seeds, mounted on slides and incubated with the TMRM probe for 5 min. Images were taken on a fluorescence confocal microscope, with 40 \times oil objective. Percentages in panels B, D, F, H and J indicate proportion of embryos in those stages, within a *calca1ca2CA2* silique. (I) Image of a cotyledon from a WT embryo in green cotyledon stage. Fluorescence intensity was measured from pictures using Image J software. Bars, 50 μ m. HAP, hours after pollination. a,b indicate significant statistically differences by *t*-test ($P < 0.05$).

calca1ca2CA2 developing siliques) or embryos from single *cal* or *ca2* mutant plants show levels of fluorescence similar to WT embryos (Supplementary Fig. S3). These results indicate that lack of CA1 and CA2 proteins results in dysfunctional mitochondria as embryo development proceeds, a situation that might be starting only at 48 HAP.

To further analyze the activity of mitochondria, a second probe was used. MitoTracker Red (Invitrogen) is a probe usually used to detect mitochondria. However, its accumulation is dependent upon membrane potential (Tal *et al.*, 2009). Thus, red fluorescence is an indication of active mitochondria. When *calca1ca2CA2* siliques were analyzed, delayed embryos corresponding to *calca2* mutants contain less active mitochondria (~30%) than WT embryos, but only at 48 HAP (Fig. 5), which is consistent with the results obtained with the TMRM probe. Immediately after pollination and until the globular stage, double knockout and WT embryos are indistinguishable.

These results suggest that the lack of CA1 and CA2 proteins might impair the electron transport chain (ETC) function. However, cells are still able to generate a mitochondrial membrane potential capable of sustaining early embryo development until at least late globular stage.

Delayed embryos show increased ROS levels

The mitochondrial respiratory chain is a major source of reactive oxygen species (ROS) in eukaryotic cells. Mitochondrial ROS production associated with a dysfunction of ETC has been implicated in a number of degenerative diseases and stresses in many organisms (Jie *et al.*, 2013). Recent findings suggest that mitochondrial ROS can be integral components of cellular signal transduction as well (Dröse and Brandt, 2012; Martin *et al.*, 2013, 2014). Within the respiratory chain, complexes I and III (ubiquinol:cytochrome c oxidoreductase) are generally considered as the main producers of superoxide anions that are released into the mitochondrial matrix and the intermembrane space, respectively. The dramatic loss of mitochondrial membrane potential observed in delayed *calca2* embryos might be a secondary effect, most likely due to accumulation of ROS. To test this hypothesis, ROS levels and distribution were studied in WT as well as in *calca1ca2CA2* siliques at different hours after controlled pollination.

Mitochondrial superoxide levels were studied using MitoSOX red (Molecular Probes). This probe is a mitochondrial superoxide indicator that is selectively targeted to mitochondria and fluoresces red upon oxidation (Robinson *et al.*,

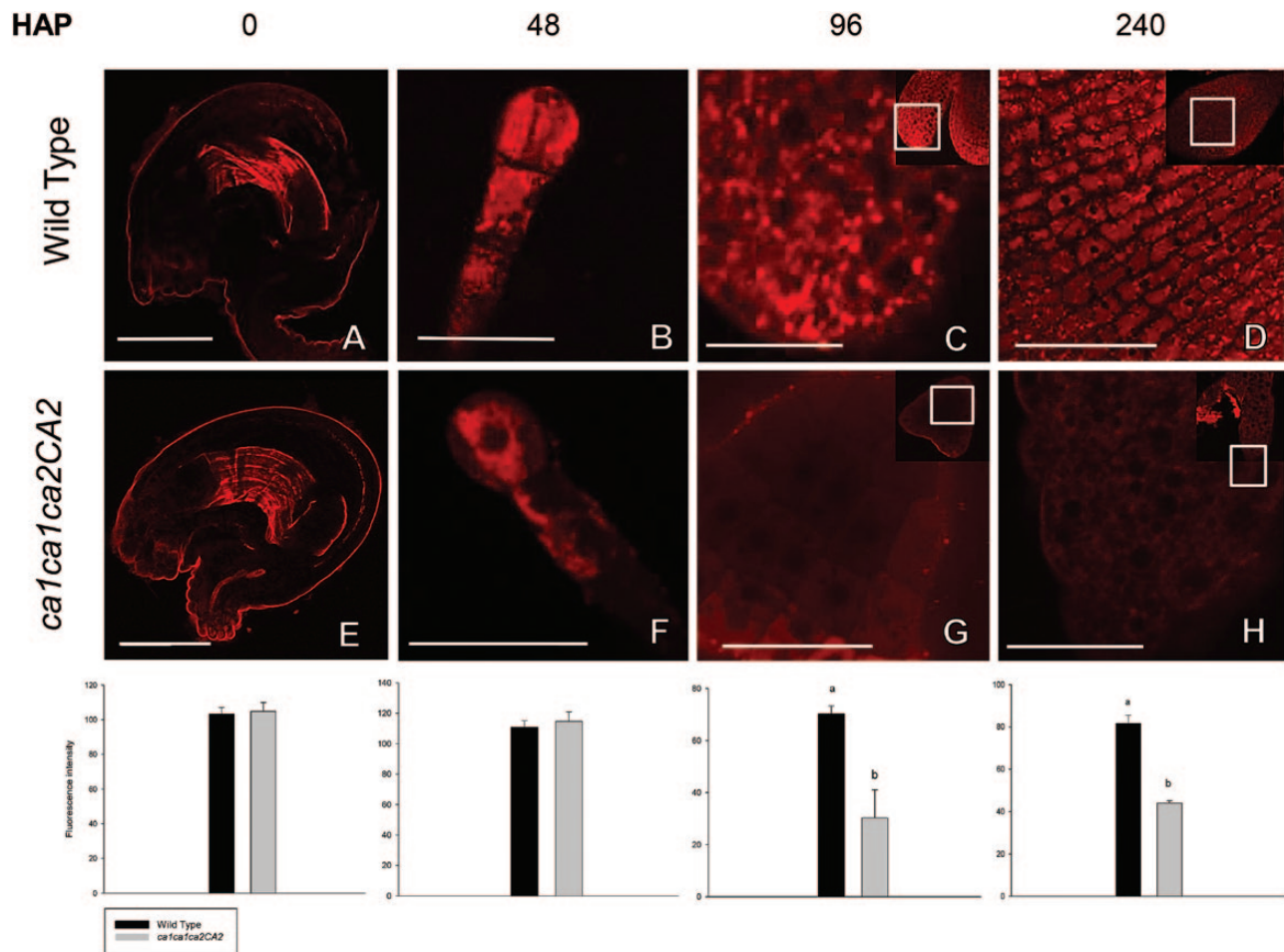


Fig. 5. Double knockout embryos contain less active mitochondria. WT and *ca1ca1ca2CA2* flowers were emasculated and manually pollinated. After the indicated time, seeds were opened and embryos were incubated on slides with Mitotracker Red. Images were taken with fluorescence confocal microscope using 40x oil objective. Fluorescence intensity was measured from pictures using Image J software. Bars: A, E and D, 50 μ m; B, C, F, G and H: 25 μ m. a, b indicate significant statistically differences by *t*-test ($P < 0.05$).

2006). The fluorescent probe 5-(and 6)-carboxy-2,7-dichlorodihydrofluorescein diacetate (H₂CDFDA; Molecular Probes) was used to analyze hydrogen peroxide levels. This probe diffuses into living cells and is rapidly hydrolyzed to 2,7-dichlorofluorescein (DCFH) and preferentially oxidized mainly by hydrogen peroxides inside the cells to the highly green fluorescent 2,7-dichlorofluorescein (DCF) (Zhang *et al.*, 2009; Bi *et al.*, 2012). Thus, DCF fluorescence is correlated with peroxide levels (Myhre *et al.*, 2003).

When WT pistils were incubated with MitoSOX, a slight signal was detected at 0 HAP and 24 HAP at the central cell zone of the embryo sac and in the developing endosperm, respectively (Fig. 6A, B), diminishing at torpedo stage until no signal was observed later in development, indicating that healthy embryos do not produce large amounts of mitochondrial

superoxide (Fig. 6C, D, E). When *calca1ca2CA2* pistils were analyzed, no differences for MitoSOX signal were detected until 24 HAP (Fig. 6F, G). However, when MitoSOX signal was analyzed in *calca1ca2CA2* pistils at later stages, the signal increases only in delayed double mutant *calca2* embryos leading to a strong red signal at the heart stage (96 HAP) that continues to be high at 240 HAP, indicating a strong production of mitochondrial superoxide (Fig. 6H, I). Similar results were obtained by using H₂CDFDA (Fig. 6J–R), indicating that delayed embryos accumulate large amounts of mitochondrial superoxide and hydrogen peroxide leading to a strong oxidative environment.

To further investigate the nature of the ROS present in the embryos, both WT and *calca1ca2CA2* siliques at different stages were incubated with NBT to look for cytosolic

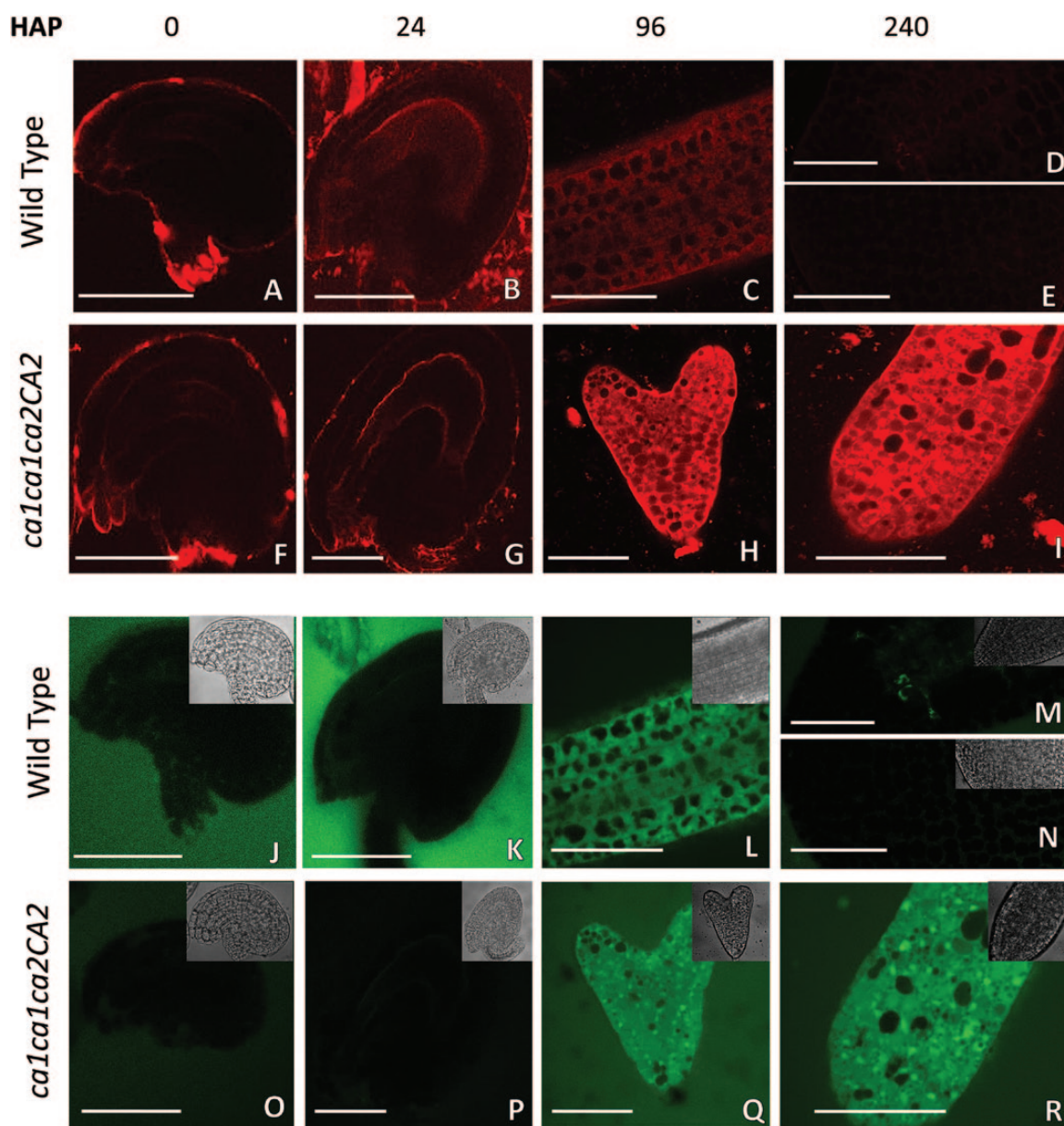


Fig. 6. Double knockout embryos accumulate mitochondrial superoxide and hydrogen peroxide. WT and *calca1ca2CA2* flowers were emasculated and manually pollinated. At the indicated time, ovules or isolated embryos were mounted on slides in presence of MitoSOX to detect mitochondrial superoxide (A–I), and H₂DCFDA detect hydrogen peroxide (J–R) and observed immediately under fluorescence confocal microscope with both channels. Bars, 50 μm.

superoxide, and with DAB to detect H₂O₂. Cytosolic superoxide was detected outside the embryo sac in ovules from unpollinated and pollinated WT pistils (48 HAP), at the micropylar end of the inner integument (Supplementary Fig. S4A, B, E, F). Later in embryogenesis, no NBT signal was observed in WT developing seeds. However, a strong signal was detected in delayed double mutant embryos (Supplementary Fig. S4G, H) indicating that not only mitochondrial superoxides are produced in the mutant embryos but also other types of superoxides as well. In the case of the DAB probe, peroxides were detected in the central cell zone of mature embryo sacs, both from WT and *calca1ca2CA2* pistils and after fertilization (24 HAP) (Supplementary Fig. S4I, J, M, N). Similar to the results obtained with NBT, strong DAB signals were detected only in delayed double mutant embryos (Supplementary Fig. S4O, P). These results reveal that the lack of CA1 and CA2 produces a strong impairment of respiration and different kinds of ROS accumulation.

Double mutant seedlings are unable to survive

As described above, ~23% of the seeds obtained by selfing *calca1ca2CA2* or *calCA1ca2ca2* plants are dark brown and wrinkled seeds (Fig. 1). To know whether these abnormal seeds are able to germinate, they were planted on MS medium together with WT or heterozygous *calca1ca2CA2* seeds. Dark brown seeds germinated 12 d later than WT or heterozygous seeds (Supplementary Fig. S5) and were severely delayed in vegetative development, undergoing a complete de-greening 2 d after (Supplementary Fig. S5). Small seedlings were analyzed by PCR and found to be homozygous for both *cal1* and *ca2* ($n=15$; Supplementary Fig. S2), whereas normal green seedlings are WT or heterozygous for either *CA1* or *CA2* ($n=10$). Thus, we conclude that *calca2* double knockout mutants are unable to develop further. These small seedlings were subjected to staining with NBT and DAB and compared with WT or *calca1ca2CA2* seedlings at approximately the same developmental stage. WT or heterozygous seedlings show low levels of superoxide and peroxide production, with high staining restricted to the root tips (Supplementary Fig. S6, left panels). In contrast, double homozygous mutant seedlings show a strong staining for both, DAB and NBT probes, indicating high ROS accumulation over the entire seedling (Supplementary Fig. S6, right panels).

Additionally, WT and wrinkled seeds or green and white immature embryos were cultivated on MS medium supplemented with Gamborg's vitamins and 3%, 5% and 8% sucrose or 1 mM reduced glutathione (GSH) or 3% sucrose, 1 mM GSH. While WT seedlings develop normally, no rescue of double homozygous plants was observed.

Abnormally large oil bodies are detected in the double mutant seeds

In maturing seeds, the two later stages before dormancy of the curled torpedo embryo are greening and de-greening. Chlorophyll functions to sustain photosynthetic capacity (Borisjuk *et al.*, 2004), although photosynthetic CO₂ fixation

is low in embryos (Asokanathan *et al.*, 1997). Oilseed plants such as *Arabidopsis* accumulate lipids to supply the energy requirements before photosynthesis is established. Such lipids are generally stored as triacylglycerols (TAGs) in spherical compartments referred to as oleosomes or oil bodies (Murphy, 1990) together with the structural protein oleosins (Huang, 1992). Thus, NADPH and ATP produced during embryonic photosynthesis were proposed to be involved in fatty acid synthesis (Goffman *et al.*, 2005). The demand of ATP is postulated to be high for this process (Nakajima *et al.*, 2012).

Because greening of the *calca2* double mutant embryos is not detected and mitochondrial membrane potential is impaired, it was reasoned that fatty acid synthesis could be compromised. To test this idea, WT as well as *calca1ca2CA2* siliques were subjected to neutral lipid staining using Nile red, which is a red dye used to specifically detect oil bodies and membranes (Siloto *et al.*, 2006; Miquel *et al.*, 2014). WT or heterozygous embryos present strong red staining, showing a large number of oil bodies inside the cells (32 ± 7 per 100 μm^2 , $n=10$). At early torpedo stage, double homozygous mutant embryos contain fewer oil bodies but are slightly larger than WT embryos (24 ± 2 per 100 μm^2 , $n=10$; Fig. 7A, D). At late torpedo stage, while in WT embryos the number of oil bodies increases, double mutant embryos still present fewer and larger oil bodies (15 ± 3 per 100 μm^2 , $n=10$, $P < 0.001$) compared to WT embryos (Fig. 7B, E) suggesting that a significantly less surface would be available for catabolism. These results reveal that a strong deficiency in complex I affects oil storage. After imbibition, WT oil bodies are almost consumed after 48 h (Fig. 7C, F). However, in the double mutants oil bodies remain, suggesting that respiration is fully compromised and unable to consume reserves to sustain sporophytic growth.

CA1 and CA2 proteins do not interact

It was hypothesized that the CA domain is composed of three subunits (trimers): two CA-type proteins and one CAL protein (Perales *et al.*, 2004). In order to investigate if both CA1 and CA2 proteins could be present in the same CA domain, a yeast two-hybrid assay was performed using the classic GAL4 system (see *Materials and methods*). While both CA1 and CA2 could form homodimers, they do not show any interaction between them (Supplementary Fig. S7). This result suggests that two conformations of complex I might co-exist *in vivo*: complex I containing CA2-dependent trimers and complex I containing CA1-dependent trimers. Since the CA2 protein is more abundant than CA1 (Klodmann *et al.*, 2010), complex I containing CA2 should be more abundant as well. This idea is consistent with the 20% remaining complex I present in *ca2* knockout mutant (Perales *et al.*, 2005).

Silencing both CA1 and CA2 genes leads to low levels of complex I

Since we were unable to obtain a double homozygous line lacking both CA1 and CA2 proteins, a strategy of silencing was undertaken using artificial microRNAs (amiRs). Two

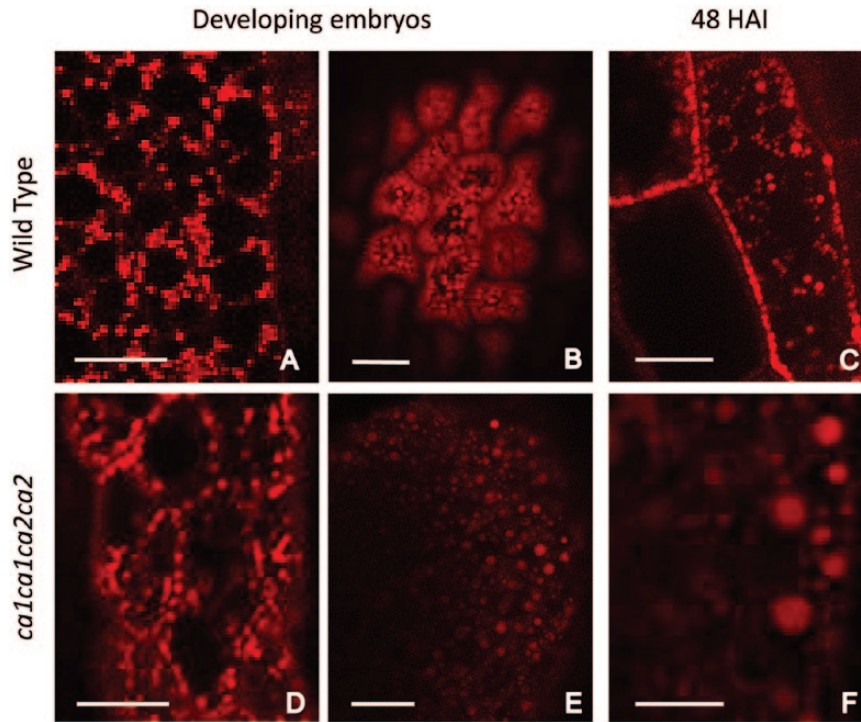


Fig. 7. Delayed *ca1ca2* embryos show bigger oil bodies. Neutral lipids stored in oil bodies were stained in WT and *ca1ca1ca2ca2* embryos by using Nile Red. At the early torpedo stage, mutant embryo oil bodies are similar in number and size to those of the WT (A and D). However, before drying, oil bodies in mutant embryos are larger and fewer in number than those in the WT (B and E). Oil bodies are larger than before in dry seeds imbibed for 48 h, while in WT they are smaller and less conspicuous (C and F). Bars, 10 μ m. HAI, hours after imbibition. (This figure is available in colour at JXB online.)

independent T-DNA constructs containing an amiR targeting both *CA1* and *CA2* messengers (*amiRca1ca2*) driven by the 35S promoter were introduced into a *rdr6* Arabidopsis background, which avoids RDR6-mediated post-transcriptional gene silencing (PTGS) of transgenes (Pontes *et al.*, 2013). Several lines were obtained with different degrees of silencing. Three independent lines with good scores of silencing were chosen for further analysis. The *CA1* and *CA2* transcript levels were detected at 2% and 14% of those of the WT, respectively (Supplementary Fig. S8A). These *amiRca1ca2* plants grow normally on MS medium or soil; however they show short stamens that hinder the fertilization process (Supplementary Fig. S8B). Nevertheless, some seeds are obtained and stable lines with strikingly similar silencing rates were established.

To explore the effect of silencing both *CA* genes on respiratory complex levels, especially complex I, organelle membranes were isolated and then the corresponding proteins separated by BN-PAGE and in-gel NADH activity was measured (see *Materials and methods*). As shown in Fig. 8B, NADH dehydrogenase activity is reduced in *amiRca1ca2* plants compared to *ca2* mutants, which contain ~20% of this complex (Perales *et al.*, 2005). All other complexes appear to be unaffected. We conclude that the reduction of both *CA* proteins strongly affects complex I levels.

Discussion

In this report, we show that the lack of two *CA* subunits of the respiratory complex I causes a strong

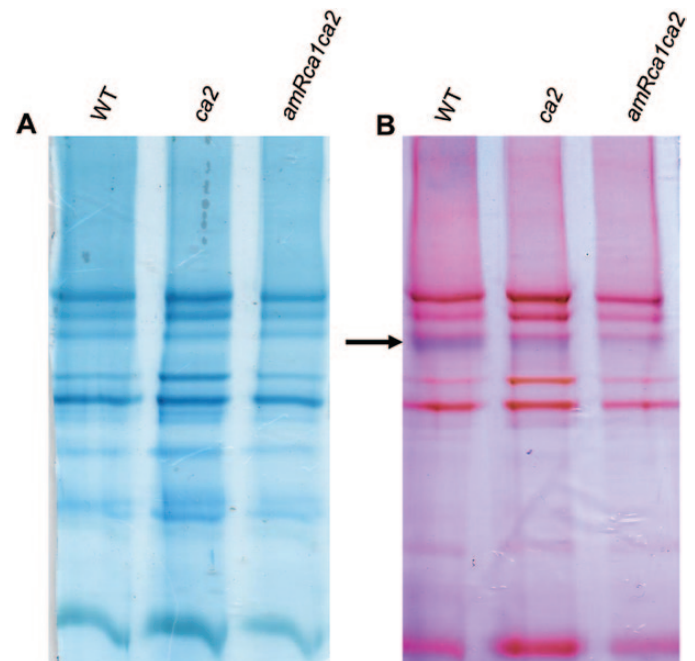


Fig. 8. *amiRca1ca2* plants contain lower levels of CI than *ca2* and WT plants. Organelle membranes were isolated from WT, *ca2* and *amiRca1ca2* lines. Protein complexes were separated by one-dimensional blue native PAGE. Gels were either (A) Coomassie-stained, or (B) analyzed for CI activity, arrowed. (This figure is available in colour at JXB online.)

reduction in mitochondrial membrane potential that leads to a lethal phenotype. Double mutant embryos are able to grow and show a normal mitochondrial membrane potential

until late globular stage, after which mutant embryos are delayed in development but continue to grow slowly. Due to extremely low membrane potential, different kinds of ROS (mitochondrial and cytoplasmic superoxides and peroxides) are accumulated, most likely further affecting electron transport chain and probably other important processes in the embryo. These embryos never reach the greening stage and consequently oil storage is lower than normal. Nevertheless, seeds are produced but they show abnormal shape and color. These dark brown seeds are able to germinate, but do so 12 d after WT seeds, most likely because of less energy supply (less oil body accessibility due to lower surface area/volume ratio, oxidative stress and impaired respiration). Severely affected seedlings contain high levels of ROS and turn white 2–3 d later and die. For these reasons, lack of CA1 and CA2 is considered lethal.

There is a large number of mutants showing embryo lethal phenotypes (Meinke *et al.*, 2008). Muralla *et al.* (2011) presented an updated, comprehensive dataset of 396 embryo defective (EMB) loci in Arabidopsis, with different phenotypes and times of developmental arrest. Several embryo defective mutants show delay or arrest in the transition from globular stage to early heart stage with a final phenotype defined as the cotyledon stage (Muralla *et al.*, 2011; Lloyd and Meinke, 2012). This particular moment of development that includes a change in symmetry from radial to bilateral is critical and certainly might be a high-energy demanding process. Several reports documented that mutants strongly affecting the respiratory chain in Arabidopsis show similar phenotypes [Welchen *et al.* (2012) for Cytc; Dahan *et al.* (2014) for CIV; Mansilla *et al.* (2015) for COX 10; this work for CI] displaying delayed growth after the globular stage. Kühn *et al.* (2015) reported a mutant named *ndufv1* which lacks NADH dehydrogenase activity of Complex I. This mutant requires sucrose to survive, thus, in normal conditions is lethal although no delay in embryogenesis was reported. The difference in the strength of the phenotype could be most likely due to the fact that in the *ndufv1* mutant, CI assembly intermediates or subcomplexes are accumulated (for example the entire membrane arm containing the CA domain). On the contrary, in *calca2* mutants no intermediate should accumulate because the defect in the biogenesis is in the very first steps.

In Arabidopsis, as in most plants, the triploid endosperm derives from the fertilization of a second sperm cell and the homo diploid (2n) central cell of the embryo sac (Sundaresan and Alandete Saez, 2010) which functions as a nutritive source for the embryo or the germinating seedling. The genotype of the endosperm is the same as the zygote. Thus, if the zygote is unable to maintain a normal mitochondrial membrane potential, it is unlikely that the endosperm could do so. In our experiments, we incubated isolated small embryos with different fluorescent probes because it was difficult to observe fluorescence in the entire developing seed under the confocal microscope. For some contaminations with endosperm cells, we observed a similar stain as in the embryo cells; however this aspect needs further investigation.

Possible composition of the CA domain

Since it was proposed that the CA domain of complex I is composed of trimers of related proteins, most likely two CA proteins and one CAL protein (Perales *et al.*, 2004; Braun *et al.*, 2014) and CA1 and CA2 do not interact (this work), it is tempting to speculate that trimers might be formed by two subunits of CA2 and one CAL (the majority of complex Is, ~80%) but also by two subunits of CA1 and one CAL (~20%). Thus, in the *ca2* mutant, the first domain is unable to form and cannot undergo complex I assembly, with the remaining 20% of the domain depending on the CA1 to form complex I. In the *cal* mutant, CA2 could form all the trimers and no differences are apparent compared to WT. In silencing *amiRcalca2* plants, complex I was much reduced (this work). In the double mutants *calca2* or *callcal2* (Wang *et al.*, 2012), we predict that none of the CA domain could be formed, complex I assembly could not take place, and as a consequence, embryogenesis is severely compromised. This prediction is consistent with the findings that rescued *calca2* plants contain no detectable assembled complex I (Hans Peter Braun, personal communication). Conversely, when CA2 is lacking and CAL proteins are strongly reduced as in *ca2cal2* or *ca2cal1* double mutants (Soto *et al.*, 2015), 20% of the complex could be formed but is not fully functional leading to an altered photorespiratory phenotype. A model is presented in Fig. 9. The comparison of phenotypes shown by different combinations of mutants reveals that two CAs and one CAL subunit are required for complex I assembly consistent with the absolute conservation of both types of subunits (Perales *et al.*, 2004). In an Arabidopsis interactome map published recently (Braun *et al.*, 2011), it is shown that CA1 and CA2 proteins interact, however, direct evidence for the CA1-CA2 interaction so far is weak. The remaining CA3 protein, which is very similar to the CA1 protein but slightly smaller, was not found in an isolated CA domain although it is present within complex I (Klodmann *et al.*, 2010). The exact localization of the CA3 protein remains elusive and needs further investigation.

Is complex I necessary for early embryo development?

Analyses of mitochondrial membrane potential suggest that early in development, double knockout *calca2* embryos are undistinguishable from single mutant or WT embryos. However, as shown in Figs 4, 5, membrane potential drops dramatically at late globular stage, correlating well with the developmental stage when mutant embryos start to show a growth delay.

Although *calca2* double mutants might contain no detectable assembled complex I, mutant embryos (and the corresponding mutant female and male gametophytes) are however able to produce a normal membrane potential of their mitochondria until late globular stage. Is this because it is possible to produce a near normal mitochondrial membrane potential without complex I (mainly dependent on complex II-III-IV) until a certain stage or because there is a certain amount of complex I derived from its mother? This

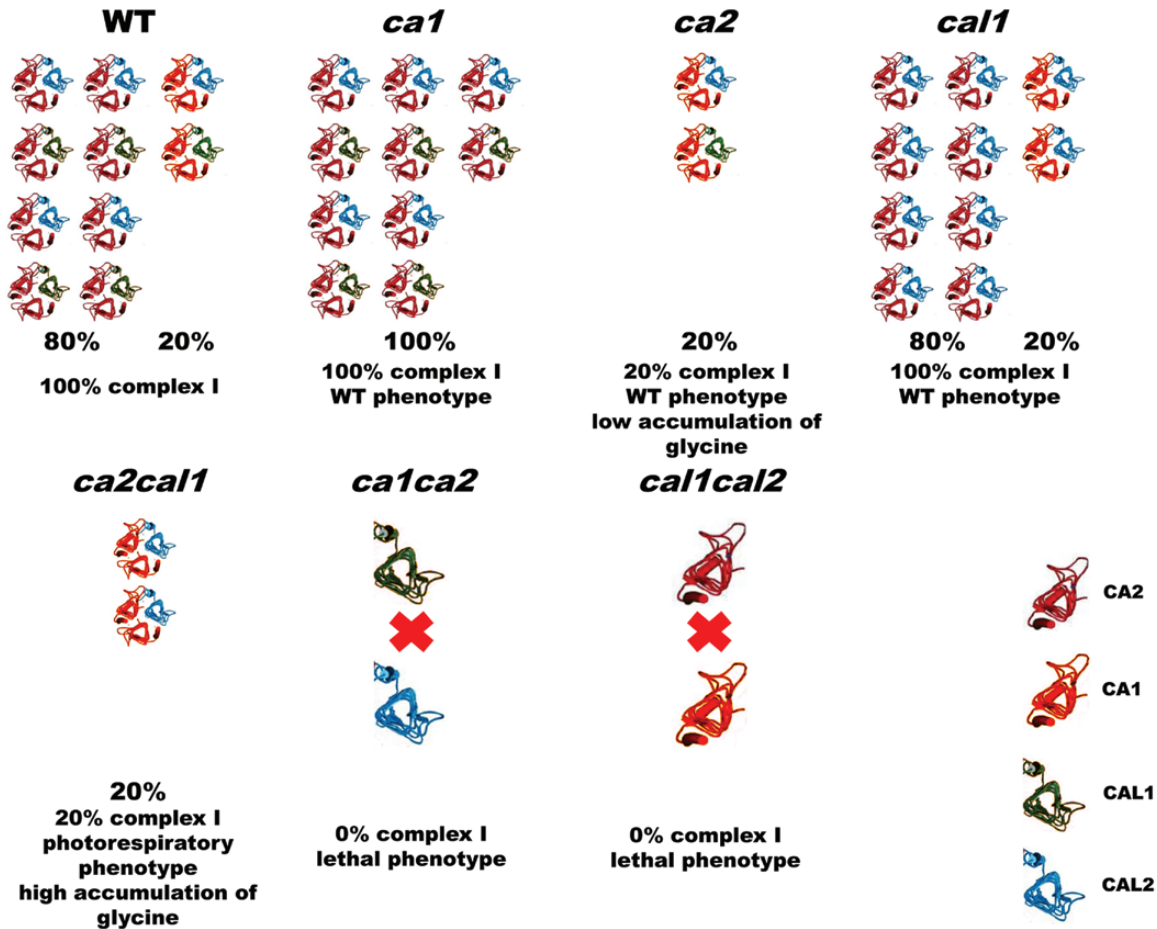


Fig. 9. Model of CA domain composition in plants. WT plants contain 80% CA2-dependent trimers, approximately half with CAL1 and half with CAL2 proteins that enable complex I assembly. The remaining 20% of the domain is dependent on CA1 protein and forms complex I. In *ca1* mutants, CA2 is able to replace CA1 and forms 100% of CA2-dependent trimers either with CAL1 or CAL2 proteins (unpublished). Thus, *ca1* plants contain 100% complex I and show WT phenotype. In *ca2* mutants (Perales *et al.*, 2005), CA1 forms trimers with CAL1 or CAL2 proteins and accounts for the 20% of complex I detected in these mutants, showing a WT phenotype although there is a low accumulation of glycine (Soto *et al.*, 2015). In *cal1* (and *cal2*) mutants (Wang *et al.*, 2012), CA2- and CA1-dependent trimers are formed with CAL1 or CAL2 and plants show the WT phenotype with 100% of complex I. In *ca2cal1* plants (Soto *et al.*, 2015), CA1 is able to form trimers with the CAL2 protein and only around 20% of complex I is assembled. Plants show a photorespiratory phenotype with high accumulation of glycine. In *ca1ca2* mutants (this work), CAL1 and CAL2 proteins are unable to interact and cannot form active trimers, thus, complex I cannot assemble and double knockouts show a lethal phenotype. In *cal1cal2* mutants (Wang *et al.*, 2012), which show a lethal phenotype, CA1 and CA2 protein do not interact (this work), and thus it is predicted that no complex I is assembled. In this case, CA1 or CA2 could not form homotrimers as they do *in vitro* (Martin *et al.*, 2009) or homotrimers are inactive *in vivo*. The *cal1cal2i* plants show 5–10% of complex I (Fromm *et al.*, 2015) which suggests that homotrimers are prohibited *in vivo*. (This figure is available in colour at *JXB* online.)

is an interesting question that needs further investigation to answer. According to published data (Li *et al.*, 2013) the CA domain shows a relatively high turnover rate. In this case, it seems unlikely that mitochondria containing complex I from the mother of the megaspore cell (sporocyte), then inherited by the functional megaspore (initial of female gametophyte), then in the egg cell (and/or central cell) and finally in the zygote (and the endosperm) could comprise proteins or messengers from the mother until late globular stage after so many cell divisions.

Conclusions

In this work, using a combination of insertional mutants in *CA* genes, we show that lack of CA1 and CA2 subunits of the complex I causes a lethal phenotype characterized by

accumulation of ROS and a strong reduction in mitochondrial membrane potential suggesting low respiration. This feature is detected after the globular stage of embryo development causing growth delay producing abnormal dark brown seeds. Since CA2 is required for 80% of complex I assembly, we predict that CA1 is required for the remaining 20%, suggesting that different types of complex I exist *in vivo*.

Supplementary data

Supplementary data are available at *JXB* online.

Figure S1. Double heterozygous mutant siliques contain abnormal, easily recognized seeds.

Figure S2. Genotyping of mutant plants and embryos.

Figure S3. Mitochondrial membrane potential in *cal1cal2CA2CA2* embryos is similar to the WT.

Figure S4. Reactive oxygen species are accumulated in *calca2* delayed embryos.

Figure S5. Double knockout *calca2* late germinating seedlings accumulate large amounts of ROS.

Figure S6. Double knockout *calca2* seeds germinate twelve days later than normal.

Figure S7. CA1 and CA2 proteins do not interact.

Figure S8. *amiRcalca2* plants show reduced fertility.

Accession numbers

Sequence data from this article can be found in the Arabidopsis Genome Initiative or GenBank/EMBL databases under the following accession numbers: Arabidopsis CA1 (At1g19580), Arabidopsis CA2 (At1g47260), Arabidopsis CAL1 (At5g63510), Arabidopsis CAL2 (At3g48680).

Acknowledgments

JPC and FM are doctoral fellows of the Consejo Nacional de Investigaciones Científicas y Técnicas (CONICET), DS is a doctoral fellow of the Universidad Nacional de Mar del Plata (UNMdP), and MVM, GCP, and EZ are CONICET researchers. EZ and GCP designed the research, JPC, FM, DS and MVM performed the experiments, EZ, JPC, MVM and GCP analyzed data, and EZ, JPC and GCP wrote the paper. We are grateful to Daniela Villamonte for excellent technical assistance with confocal microscopy. This research was funded by Agencia Nacional de Promoción Científica y Técnica (ANPCyT), CONICET and the Howard Hughes Medical Institute (HHMI).

References

- Andrews B, Carroll J, Ding S, Fearnley IM, Walker JE.** 2013. Assembly factors for the membrane arm of human complex I. *Proceeding of the National Academy of Sciences, USA* **110**, 18934–18939.
- Asokanthan P, Johnson W, Griffith M, Krol M.** 1997. The photosynthetic potential of canola embryos. *Physiologia Plantarum* . **101**, 353–360.
- Bi Y, Chen W, Zhang W, Zhou Q, Yun L, Xing D.** 2012. Production of reactive oxygen species, impairment of photosynthetic function and dynamic changes in mitochondria are early events in cadmium-induced cell death in *Arabidopsis thaliana*. *Biology of the Cell* **101**, 629–643.
- Borisjuk L, Rolletschek H, Radchuk R, Weschke W, Wobus U, Weber H.** 2004. Seed development and differentiation: a role for metabolic regulation. *Plant Biology* **6**, 375–386.
- Bowman JL, Mansfield SG, Koorneef, M.** 1994. Embryogenesis in *Arabidopsis*: an atlas of morphology and development. In: Bowman, J ed. Springer-Verlag, 349–401.
- Brand MD, Nicholls DG.** 2011. Assessing mitochondrial dysfunction in cells. *Biochemical Journal* . **435**, 297–312.
- Braun HP, Binder S, Brennicke A, et al.** 2014. The life of plant mitochondrial complex I. *Mitochondrion* **19**, 295–313.
- Braun HP, Zabaleta E.** 2007. Carbonic anhydrase subunits of the mitochondrial NADH dehydrogenase complex (complex I) in plants. *Physiologia Plantarum* . **129**, 114–122.
- Braun P, Carvunis AR, Charlotteaux B, et al.** [The Arabidopsis Interactome Mapping Consortium]. 2011. Evidence for network evolution in an Arabidopsis interactome map. *Science* **333**, 601–607.
- Bridges HR, Fearnley IM, Hirst J.** 2010. The subunit composition of mitochondrial NADH:ubiquinone oxidoreductase (complex I) from *Pichia pastoris*. *Molecular Cell Proteomics* **9**, 2318–2326.
- Cardol P.** 2011. Mitochondrial NADH:ubiquinone oxidoreductase (complex I) in eukaryotes: a highly conserved subunit composition highlighted by mining of protein databases. *Biochimica et Biophysica Acta (BBA) - Bioenergetics* **1807**, 1390–1397.
- Clough SJ, Bent AF.** 1998. Floral dip: a simplified method for *Agrobacterium*-mediated transformation of *Arabidopsis thaliana*. *The Plant Journal* **16**, 735–743.
- Colas des Francs-Small C, Small I.** 2014. Surrogate mutants for studying mitochondrially encoded functions. *Biochimie* **100**, 234–42.
- Dahan J, Tcherkez G, Macherel D, Benamar A, Belcram K, Quadrado M, Arnal N, Mireau H.** 2014. Disruption of the CYTOCHROME C OXIDASE DEFICIENT1 gene leads to cytochrome c oxidase depletion and reorchestrated respiratory metabolism in *Arabidopsis*. *Plant Physiology* **166**, 1788–1802.
- de Longevialle AF, Meyer EH, Andrés C, Taylor NL, Lurin C, Millar AH, Small ID.** 2007. The pentatricopeptide repeat gene OTP43 is required for trans-splicing of the mitochondrial *nad1* Intron 1 in *Arabidopsis thaliana*. *Plant Cell* **19**, 3256–3265.
- Dröse S, Brandt U.** 2012. Molecular mechanisms of superoxide production by the mitochondrial respiratory chain. *Advances in Experimental Medicine and Biology* . **748**, 145–169.
- Dudkina NV, Eubel H, Keegstra W, Boekema EJ, Braun HP.** 2005. Structure of a mitochondrial supercomplex formed by respiratory-chain complexes I and III. *Proceeding of the National Academy of Sciences, USA* **102**, 3225–3229.
- Dutilleul C, Driscoll S, Cornic G, De Paepe R, Foyer CH, Noctor G.** 2003. Functional mitochondrial complex I is required by tobacco leaves for optimal photosynthetic performance in photorespiratory conditions and during transients. *Plant Physiology* **131**, 264–275.
- Eubel H, Jansch L, Braun HP.** 2003. New insights into the respiratory chain of plant mitochondria. Supercomplexes and a unique composition of complex II. *Plant Physiology* **133**, 274–286.
- Friedrich T.** 1998. The NADH:ubiquinone oxidoreductase (complex I) from *Escherichia coli*. *Biochimica et Biophysica Acta (BBA)* **1364**, 134–146.
- Fromm S, Göing J, Lorenz C, Peterhänsel C, Braun HP.** 2015. Depletion of the 'gamma-type carbonic anhydrase-like' subunits of complex I affects central mitochondrial metabolism in *Arabidopsis thaliana*. *Biochimica et Biophysica Acta (BBA)* **1857**, 60–71.
- Gawryluk RM, Gray MW.** 2010. Evidence for an early evolutionary emergence of gamma-type carbonic anhydrases as components of mitochondrial respiratory complex I. *BMC Evolutionary Biology* **10**, 176. doi: 10.1186/1471-2148-10-176
- Gietz D, St Jean A, Woods A, Schiestl, R.** 1992. Improved method for high efficiency transformation of intact yeast cells. *Nucleic Acids Research* **20**, 1425.
- Goffman FD, Alonso AP, Schwender J, Shachar-Hill Y, Ohlrogge JB.** 2005. Light enables a very high efficiency of carbon storage in developing embryos of rapeseed. *Plant Physiology* **138**, 2269–2279.
- Gray MW.** 2012. Mitochondrial evolution. *Cold Spring Harbour Perspective Biology* , **4**, a011403.
- Haïli N, Arnal N, Quadrado M, Amiar S, Tcherkez G, Dahan J, Briozzo P, Colas des Francs-Small C, Vrielynck N, Mireau H.** 2013. The pentatricopeptide repeat MTSF1 protein stabilizes the *nad4* mRNA in *Arabidopsis* mitochondria. *Nucleic Acids Research* . **41**, 6650–6663.
- Heazlewood JL, Howell KA, Millar AH.** 2003. Mitochondrial complex I from *Arabidopsis* and rice: orthologs of mammalian and fungal components coupled with plant-specific subunits. *Biochimica et Biophysica Acta (BBA)* **1604**, 159–169.
- Huang AHC.** 1992. Oil bodies and oleosins in seeds. *Annual Review of Plant Physiology and Plant Molecular Biology* **43**, 177–200.
- Jie L, Wuliji O, Wei Li, Zhi-Gang Jiang, Ghanbari HA.** 2013. Oxidative stress and neurodegenerative disorders. *International Journal of Molecular Science* **14**, 24438–24475.
- Karpova OV, Newton KJ.** 1999. A partially assembled complex I in NAD4-deficient mitochondria of maize. *The Plant Journal* **17**, 511–521.
- Klodmann J, Sunderhaus S, Nitz M, Jansch L, Braun HP.** 2010. Internal architecture of mitochondrial complex I from *Arabidopsis thaliana*. *The Plant Cell* **22**, 797–810.
- Kühn K, Obata T, Feher K, Bock R, Fernie AR, Meyer EH.** 2015. Complete mitochondrial complex I deficiency induces an up-regulation of respiratory fluxes that is abolished by traces of functional complex I. *Plant Physiology* **168**, 1537–1549.
- Li L, Nelson CJ, Carrie C, Gawryluk RM, Solheim C, Gray MW, Whelan J, Millar AH.** 2013. Subcomplexes of ancestral respiratory complex I subunits rapidly turn over *in vivo* as productive assembly intermediates in *Arabidopsis*. *Journal of Biological Chemistry* **288**, 5707–5717.

- Lloyd J, Meinke D.** 2012. A comprehensive dataset of genes with a loss-of-function mutant phenotype in *Arabidopsis thaliana*. *Plant Physiology* **158**, 1115–1129.
- Mansilla N, García L, González DH, Welchen E.** 2015. AtCOX10, a protein involved in haem o synthesis during cytochrome c oxidase biogenesis, is essential for plant embryogenesis and modulates the progression of senescence. *Journal of Experimental Botany* doi: 10.1093/jxb/erv381.
- Martin MV, Distéfano AM, Bellido A, Córdoba JP, Soto D, Pagnussat GC, Zabaleta E.** 2014. Role of mitochondria during female gametophyte development and fertilization in *A. thaliana*. *Mitochondrion*, **B**, 350–536.
- Martin MV, Fiol DF, Sundaresan V, Zabaleta E, Pagnussat GC.** 2013. *oiva*, a female gametophytic mutant impaired in a mitochondrial manganese-superoxide dismutase, reveals crucial roles for reactive oxygen species during embryo sac development and fertilization in *Arabidopsis*. *The Plant Cell* **25**, 1573–1591.
- Martin MV, Villarreal F, Miras I, Navaza A, Haouz A, González-Lebrero RM, Kaufman SB, Zabaleta E.** 2009. Recombinant plant gamma carbonic anhydrase homotrimers bind inorganic carbon. *FEBS Letters* **583**, 3425–3430.
- Meinke D.** 1994. Seed development in *Arabidopsis thaliana*. In: Somerville CR, Meyerowitz EM, eds. *Arabidopsis*. Cold Spring Harbor, NY: Cold Spring Harbor Laboratory Press, 253–295.
- Meinke D, Muralla R, Sweeney C, Dickerman A.** 2008. Identifying essential genes in *Arabidopsis thaliana*. *Trends in Plant Science* **13**, 483–491.
- Meyer EH, Solheim C, Tanz SK, Bonnard G, Millar AH.** 2011. Insights into the composition and assembly of the membrane arm of plant complex I through analysis of subcomplexes in *Arabidopsis* mutant lines. *Journal of Biological Chemistry* **286**, 26081–26092.
- Meyer EH, Tomaz T, Carroll AJ, Estavillo G, Delannoy E, Tanz SK, Small ID, Pogson BJ, Millar AH.** 2009. Remodeled respiration in *ndufs4* with low phosphorylation efficiency suppresses *Arabidopsis* germination and growth and alters control of metabolism at night. *Plant Physiology* **151**, 603–619.
- Miquel M, Trigui T, d'Andréa S, Kelemen Z, Baud S, Berger A, Deruyffelaere C, Trubuil A, Lepiniec L, Dubreucq B.** 2014. Specialization of Oleosins in oil body dynamics during seed development in *Arabidopsis* seeds. *Plant Physiology* **164**, 1866–1878.
- Mortensen M, Ferguson DJ, Edelmann M, Kessler B, Morten KJ, Komatsu M, Simon AK.** 2010. Loss of autophagy in erythroid cells leads to defective removal of mitochondria and severe anemia *in vivo*. *Proceeding of the National Academy of Sciences, USA* **107**, 832–837.
- Muralla R, Lloyd J, Meinke D.** 2011. Molecular foundations of reproductive lethality in *Arabidopsis thaliana*. *PLoS One* **6**:e28398. doi: 10.1371/journal.pone.0028398.
- Murphy DJ.** 1990. Storage lipid bodies in plants and other organisms. *Progress in Lipid Research* **29**, 299–324.
- Myhre O, Andersen JM, Aarnes H, Fonnum F.** 2003. Evaluation of the probes 2,7-dichlorofluorescein diacetate, luminol, and lucigenin as indicators of reactive species formation. *Biochemical Pharmacology* **65**, 1575–1582.
- Nakajima S, Ito H, Tanaka R, Tanaka A.** 2012. Chlorophyll b reductase plays an essential role in maturation and storability of *Arabidopsis* seeds. *Plant Physiology* **160**, 261–273.
- Parisi G, Perales M, Fornasari M, et al.** 2004. Gamma carbonic anhydrases in plant mitochondria. *Plant Molecular Biology* **55**, 193–207.
- Perales M, Eubel H, Heinemeyer J, Colaneri A, Zabaleta E, Braun HP.** 2005. Disruption of a nuclear gene encoding a mitochondrial gamma carbonic anhydrase reduces complex I and supercomplex I + III2 levels and alters mitochondrial physiology in *Arabidopsis*. *Journal of Molecular Biology* **350**, 263–277.
- Perales M, Parisi G, Fornasari MS, et al.** 2004. Gamma carbonic anhydrase like complex interact with plant mitochondrial complex I. *Plant Molecular Biology* **56**, 947–957.
- Peters K, Belt K, Braun HP.** 2013. 3D Gel map of *Arabidopsis* complex I. *Frontiers in Plant Science* **4**, 153 doi: 10.3389/fpls.2013.00153.
- Pineau B, Mathieu C, Gérard-Hirne C, De Paepe R, Chétrit P.** 2005. Targeting the NAD7 subunit to mitochondria restores a functional complex I and a wild-type phenotype in the *Nicotiana sylvestris* CMS II mutant lacking nad7. *Journal of Biological Chemistry* **280**, 25994–26001.
- Pineau B, Layoune O, Danon A, De Paepe R.** 2008. L-galactono-1,4-lactone dehydrogenase is required for the accumulation of plant respiratory complex I. *Journal of Biological Chemistry* **47**, 32500–32505.
- Pontes O, Vitins A, Ream TS, Hong E, Pikaard, CS and Costa-Nunes P.** 2013. Intersection of small RNA pathways in *Arabidopsis thaliana* sub-nuclear domains. *PLoS One* **8**:e65652. doi: 10.1371/journal.pone.0065652.
- Robinson KM, Janes MS, Pehar M, Monette JS, Ross MF, Hagen TM, Murphy MP, Beckman, JS.** 2006. Selective fluorescent imaging of superoxide *in vivo* using ethidium-based probes. *Proceeding of the National Academy of Sciences, USA* **103**, 15038–15043.
- Siloto R, Findlay K, Lopez-Villalobos A, Yeung EC, Nykiforuk CL, Moloney MM.** 2006. The accumulation of oleosins determines the size of seed oilbodies in *Arabidopsis*. *The Plant Cell* **18**, 1961–1974.
- Soto D, Córdoba JP, Villarreal F, Bartoli C, Schmitz J, Maurino VG, Braun HP, Pagnussat GC, Zabaleta E.** 2015. Functional characterization of mutants affected in the carbonic anhydrase domain of the respiratory complex I in *Arabidopsis thaliana*. *The Plant Journal* **83**, 831–844.
- Sundaresan V, Alandete-Saez, M.** 2010. Pattern formation in miniature: the female gametophyte of flowering plants. *Development* **137**, 179–189.
- Sunderhaus S, Dudkina NV, Jansch L, Klodmann J, Heinemeyer J, Perales M, Zabaleta E, Boekema EJ Braun HP.** 2006. Carbonic anhydrase subunits form a matrix-exposed domain attached to the membrane arm of mitochondrial complex I in plants. *Journal of Biological Chemistry* **281**, 6482–6488.
- Tal MC, Sasai M, Lee HK, Yordy B, Shadel GS, Iwasaki A.** 2009. Absence of autophagy results in reactive oxygen species-dependent amplification of RLR signaling. *Proceeding of the National Academy of Sciences, USA* **106**, 2770–2775.
- Villarreal F, Martín V, Colaneri A, González-Schain N, Perales M, Martín M, Lombardo, C, Braun HP, Bartoli C, Zabaleta E.** 2009. Ectopic expression of mitochondrial gamma carbonic anhydrase 2 causes male sterility by anther indehiscence. *Plant Molecular Biology* **70**, 471–485.
- Wang Q, Fristedt R, Yu X, Chen Z, Liu H, Lee Y, Guo H, Merchant SS, Lin C.** 2012. The γ -carbonic anhydrase subcomplex of mitochondrial complex I is essential for development and important for photomorphogenesis of *Arabidopsis*. *Plant Physiology* **160**, 1373–1383.
- Welchen E, Hildebrandt TM, Lewejohann D, Gonzalez DH, Braun HP.** 2012. Lack of cytochrome c in *Arabidopsis* decreases stability of Complex IV and modifies redox metabolism without affecting Complexes I and III. *Biochimica et Biophysica Acta (BBA)* **1817**, 990–1001.
- Wittig I, Braun HP, Schagger H.** 2006. Blue-Native PAGE. *Nature Protocols* **1**, 418–428.
- Zabaleta E, Martin MV, Braun HP.** 2012. A basal Carbon Concentrating Mechanism in Plants? *Plant Science* **187**, 94–104.
- Zhang L, Li Y, Xing D, Gao C.** 2009. Characterization of mitochondrial dynamics and subcellular localization of ROS reveal that HsfA2 alleviates oxidative damage caused by heat stress in *Arabidopsis*. *Journal of Experimental Botany* **60**, 2073–2091.